

# DARK MATTER, DISCRETENESS AND COLLISION ERROR IN COSMOLOGICAL N-BODY SIMULATIONS

Randall J. Splinter<sup>1</sup>, Adrian L. Melott<sup>2</sup>, and Sergei F. Shandarin<sup>2</sup>

randal@convex.hp.com, melott@kusmos.phsx.ukans.edu, sergei@kusmos.phsx.ukans.edu

## ABSTRACT

We report on a series of tests of agreement between three types of N-body simulations: PM, P<sup>3</sup>M, and Tree codes. We find good agreement in both the individual and the statistical properties only on scales larger than the mean interparticle separation. As a result, we question most numerical results at and below galaxy scales, either concerning primordial dark matter or baryonic matter coupled to it by gravitation.

*Subject headings:* cosmology:miscellaneous–gravitation–hydrodynamics–  
methods: numerical–dark matter

## 1. Introduction

If the dark matter in the Universe is some sort of weakly interacting particle, or even a population of primordial black holes, then artificial discreteness effects of all kinds should be thoroughly suppressed in numerical simulations of its gravitational clustering. Their contribution both to errors in the initial conditions and two-body scattering in the dynamical evolution are negligible in the Universe and therefore should be negligible in the simulation. If not, the results (including those of baryons, entrained in the gravitational field) cannot be relied upon to be consequences of physical initial conditions – regardless of whether they resemble astronomical observations.

It has been argued, based on a variety of numerical studies, that there are real problems with the HFLMR (High Force Low Mass Resolution) approach which dominates

---

<sup>1</sup>Current Address: Hewlett–Packard Company, High Performance Computing Division, 20 Perimeter Summit Blvd, MS 1904, Atlanta, GA 30319–1417

<sup>2</sup>Department of Physics and Astronomy, University of Kansas, Lawrence, KS 66045

the cosmological N–body methodology. (Peebles, et al. 1989; Melott 1990; Suisalu and Saar 1995; Kuhlman et al. 1996; Melott et al. 1997; Park 1997). It is clear from these studies that there are unphysical scattering processes taking place in HFLMR codes, but the precise effects are not clear. Recently Craig (1997), Klypin et al (1997), and Moore et al. (1997) have argued convincingly that the central regions of dark matter halos have been seriously misrepresented by numerical results due to lack of resolution. We present here some preliminary results of a much larger study (Splinter et al. 1998) which explores the limitations of mass resolution in cosmological clustering simulations.

We use PM (Hockney & Eastwood 1988; Melott 1981, 1986), AP<sup>3</sup>M (Couchman 1991), and Tree (Suginohara et al. 1991; Suto 1993) codes. The P<sup>3</sup>M code had adaptive smoothing turned off since we wish to compare a standard P<sup>3</sup>M method. The Tree runs use the fixed smoothing length in comoving coordinates, and we set a tolerance parameter  $\theta = 0.2$  which is considerably smaller (and thus more accurate) than conventional choices ( $\theta = 0.5 \sim 0.75$ ).  $\theta$  merely controls how far the tree expansion is carried, and thus the accuracy of long-range forces.

The initial power spectrum in all cases was  $P(k) \propto k^{-1}$  up to some cutoff, in most cases at the Nyquist frequency  $k = 16k_f$  dictated by the runs with the fewest particles. Realization of the corresponding density field was generated using the Zel’dovich approximation (Zel’dovich 1970) to perturb the particles from their initial lattice (Doroshkevich et al. 1980). All the models are evolved in the Einstein – de Sitter universe ( $\Omega_0 = 1$ ). The comparisons were performed at three different epochs when the nonlinear wavenumber  $k_{nl}$  becomes  $16k_f$ ,  $8k_f$ , and  $4k_f$ , where  $k_{nl} = k_{nl}(A)$  is defined as

$$\sigma^2(k_{nl}, A) = A^2 \int_0^{k_{nl}} P(k) d^3k = 1. \quad (1)$$

In the above  $A$  denotes the expansion factor (unity at the initial condition), and these values of  $k_{nl}$  correspond to the epochs  $A = 22.36$ ,  $42.13$ , and  $92.20$ , respectively. The latest moment we studied corresponds to nonlinearity on the largest scale which does not suffer from finite-volume boundary condition problems (Ryden & Gramman 1991; Kauffmann & Melott 1992). The specific runs presented here and the model parameters are shown in Table 1. We note that PM codes, which have been extensively used in most physical applications with large numbers of particles, are much faster than the other two types. Thus our  $128^3$  PM runs took much less CPU time than even the  $32^3$  Tree or P<sup>3</sup>M runs. The typical limitation on PM runs is memory or disk space, while CPU time is the typical limitation on P<sup>3</sup>M or Tree runs.  $a$  is the absolute scale of force resolution. We define  $\epsilon = a\bar{n}_{sim}^{1/3}$  so that  $\epsilon = 1$  corresponds to smoothing at the mean interparticle separation. HFLMR codes usually run with  $\epsilon < 1$ , but we will examine their behavior over a range in  $N$  and  $\epsilon$ , pushing them toward  $\epsilon = 1$  by increasing the number of particles while keeping the

absolute scale of force resolution  $a$  constant. So far as we know, this crucial experiment has not previously been done with HFLMR codes.

Our primary strategy is therefore to highlight the largely unexplored mass resolution issue by varying the number of particles while keeping  $a$  constant (it is not *exactly* constant because in fact the shape of the short-range softening function is different in all three codes). Within a given code  $a$  will be constant, so we can spot trends. Between codes softening will be of comparable size. We can define  $r_{50}$  as the radius where the force drops to 50% of the Newtonian value. For the  $P^3M$  code,  $r_{50} = 0.92a$ . For the Tree code  $r_{50} = 0.87a$ . For our PM code,  $r_{50} = 0.95$  grid unit, albeit with considerable scatter in the softened zone.

In most cases we set  $a = 1$  (in units where the box size is 128) in both the Tree and  $P^3M$  codes, and run PM with a  $128^3$  mesh. (The  $P^3M$  runs had one mesh cell per particle, but this is not the factor determining force resolution there.) It is typical of HFLMR codes to have  $a$  considerably less than  $\bar{l}_{sep}$ , the mean interparticle separation over the entire simulation box. In most uses of PM codes, the opposite is true (although in gravitational applications it has become customary to have  $\epsilon$  as small as 1 or 0.5).

It is important to note that one cannot represent initial power to higher than the Nyquist wavenumber of the particles or the mesh of the FFT used to impose the initial conditions, whichever is worse (in fact the latter is rarely the problem in cosmology). Therefore most of our runs only have initial power up to  $k_c = 16k_f$ , so that comparisons of only the effects of divergent numerical integration can be done. We show here results from a full  $128^3$  PM simulation with this power spectrum, and  $32^3$  simulations with the same *force* resolution, different mass resolution, and the same initial conditions. In order to explore the effects of having initial power at higher wave-numbers which is only possible with more particles, we have one PM run with  $k_c = 64k_f$ .

We now have for the first time a large number of runs using 3 different codes with identical initial conditions, identical force resolution, but varying mass resolution. In particular the number of particles varies widely enough to study the same physical system with values of  $\epsilon$  typical of HFLMR codes as well as to study the same system with a PM code with similar force resolution *and* matching mass resolution ( $\epsilon = 1$ ).

It is important to note time-step limitations. Elementary principles of numerical stability require that no particle move more than a fraction of a softening length  $a$ , or about one-half mesh unit for  $PM$ , in a single time-step. This condition was amply enforced for all three codes.

## 2. Results

Figure 1 shows power spectra computed on the  $128^3$  mesh appropriate to the force resolution, normalized such that a Poisson distribution with  $128^3$  particles has  $P(k) \sim 1$ . The dotted line shows the spectrum of the  $32^3$  initial conditions. It looks unusual because such spectra are not usually shown out to the force resolution scale – even though later results usually are shown to this scale. Other types of unperturbed particle arrangements than our lattice will have other features, but the overall amplitude is constrained to be similar. A full complement of  $128^3$  particles would allow the power law to continue across the plot.

It should be noted that in all HFLMR codes there are features due to particle discreteness present beyond the particle Nyquist frequency, which are resolved and evolved. Whatever the particle arrangement, they are not random phase and cannot evolve as the initial conditions do since they are tied to the particles.

Above this we see spectra for three evolved stages. The first (corresponding to the onset of nonlinearity at the mass resolution scale of the  $32^3$  particle simulations) and the last (without serious boundary condition problems) of these are shown on the left side as ratios to the power in one of them, in order to clarify differences. It can be seen that in the first of these that the spectra agree well at low  $k$  (linear theory) and very high  $k$  (pure mode coupling) frequencies, but disagree between. In the range of  $10 < k < 20$  (in units of the fundamental  $k_f$ ), there are three classes of spectra: those with  $32^3$  particles (bottom group), those with the same initial conditions but more particles (middle group) and the one which had full initial power down to  $k = 64$  (top group). There is nearly a factor of two range here. (In this and following measures we compute spectra from an initially identical  $32^3$  subset of the  $128^3$  run to suppress sampling differences). By the final stage (as evolved as is safe with periodic boundary conditions) the differences have moved to high  $k$ . If only force resolution mattered, these would be identical to  $k = 64$ . In fact, they diverge around  $k = 20$ , close to the limit set by mass resolution. We cannot say which run is correct, and we did not even find a monotonic trend with mass resolution.

An arbitrary density field is described by both the amplitudes and phases of its Fourier coefficients. We now examine the phase agreement between various codes. Figure 2 examines  $\langle \cos \theta \rangle$ , where  $\theta$  is the difference in phase angle between the same Fourier coefficient in different simulations and the average is over all wave-numbers with the same amplitude  $|k|$ . Simulations which agree have  $\langle \cos \theta \rangle = 1$ ; totally uncorrelated results have  $\langle \cos \theta \rangle = 0$ . The open circles show the  $128^3$  PM and P<sup>3</sup>M runs with identical initial conditions compared. (We do not have a  $128^3$  Tree run but results with  $64^3$  and  $32^3$  runs shown in Splinter et al. 1998 support the same trend.) The bottom group (filled squares)

shows the  $128^3$  particle PM run with full initial conditions down to  $k = 64$  compared with all other runs. In order to reduce confusion, we do not show our other results, which lie in between. Thus (a) As the number of particles are increased, with force resolution and initial conditions held constant, different codes agree better. (b) Even when they agree (given identical initial conditions), none of them agree strongly on small scales with a run that had the full range of proper initial conditions as allowed by having more particles.

In Table 2, we show the density correlation coefficient  $k_{12} = \frac{\langle \delta_1 \delta_2 \rangle}{(\sigma_1 \sigma_2)^{1/2}}$  where  $\delta$  are the density contrasts in two simulations and  $\sigma$  their RMS values. Above the diagonal we show values on the  $128^3$  mesh; below the  $32^3$  mesh. Below the diagonal, results approach  $k = 1$ , indicating near perfect agreement. Above the diagonal, again recalling that the  $k_c = 16$  PM run, the Tree, and  $P^3M$  runs have the same initial conditions, we see that these runs agree best when the  $128^3$  runs are compared. Lastly, the  $k_c = 64$  PM run does not agree strongly with any of the others. Again we conclude that integration errors are greatly reduced when more particles are included, but that the inclusion of perturbations on small scales is also important. The precise effect of ignoring them is spectrum-dependent.

### 3. Does It Matter?

The reader is referred to the center and bottom center images of Figure 7 in Beacom et al. (1991) for another example of the importance of initial power on small scales even when it is deep in the nonlinear regime. There, as well as in Melott & Shandarin (1993), we emphasized the effectiveness of the transfer of power from long to short waves. The general position and orientation of objects is determined by initial perturbations on that comoving scale and larger, so smaller perturbations are ignorable for this purpose. See also Little et al. (1991), Evrard and Crone (1992). However, here we stress that the *internal structure* of these objects will vary depending on smaller-scale perturbations. If we wish to study that internal structure, the smaller-scale initial perturbations must be present and properly evolved.

We have shown that even with nearly identical force resolution, different N-body codes differ in their results below the mean interparticle separation. They converge either by smoothing on this larger scale or by putting in more particles so that the scales are the same. Codes which give different answers cannot all be correct. On the other hand, it might be that the results on small scales are statistically equivalent, in the sense that quantities of interest computed from the ensembles are the same. This turns out not to be true. Even the autocorrelation function is affected by mass resolution; phase sensitive measures are more strongly affected. We present here only one simple set of measures, based on the mass

density.

The percolation code of Yess and Shandarin (1996) is used to identify connected regions on the  $128^3$  mesh above a given density threshold. In Figure 3 we show the ratio of total mass in regions above a given density contrast to the value found in the  $k_c = 64$  PM simulation at the first and last of our evolved stages. The situation is time-dependent and complex to describe. Clearly there are major differences, but the codes agree in low density regions. The total mass at the high density limit varies by an order of magnitude. At the earlier stage all curves were below unity in the region of  $\delta \sim 50$ , suggesting that a generation of structures were missed by the absence of correct initial conditions found only in one run. Later we find that within a code type, a higher particle density results in higher peak densities. Clearly, high density regions are not trustworthy! We found that with binning on the  $32^3$  mesh (not shown) the curves agree well; the maximum difference there is about 25%.

We have examined infall velocities and velocity dispersions (Splinter et al. 1998) and found measurable differences. All the differences we find are systematic errors, so no error bars are shown. The differences should be measured against the desired accuracy one wants to get from the computations.

We cannot easily compare our results with others, because no study has included our variety of codes, mass resolution, and inclusion of normally absent small-scale perturbations. The most similar work is the unpublished study coordinated by D.H. Weinberg. An analysis similar to our velocity studies (not shown) produced very similar results. Efstathiou et al. (1988) studied evolution of power-law initial conditions in a P<sup>3</sup>M code, using primarily low-order or averaged statistics. They did find fluctuations of order 50% in the rescaled multiplicity function (their Figure 9); while not equivalent, this is roughly compatible with the nature of our results in Figure 3.

We believe the safest course to follow is to restrict attention to scales above the mean particle separation. Given current computer technology and volumes large enough to respect boundary conditions, this implies scales of order 100 to 200 kpc. With nested-grid codes (eg. Splinter 1996) or other schemes to approximate an external zone, this may be considerably improved. However, we caution that careful testing is needed in the nonlinear regime. It is not enough to produce something that resembles our Universe; we must have confidence that it is a consequence of the initial conditions that were supposed to be modeled.

At the present time, we are quite skeptical of nearly all numerical results on early galaxy formation and the inner parts of dark matter halos, as they are typically below the

mean interparticle separation of the simulations in question.

ALM and SFS acknowledge financial support from the NSF–EPSCoR program, NASA grant NAG5-4039, and computing resources at the National Center for Supercomputing Applications. We thank Yasushi Suto for Treecode simulations permission to discuss common results.

## REFERENCES

- Beacom, J.F., Dominik, K., Melott, A.L, Perkins, S.P., & Shandarin, S.F. 1991 ApJ 372, 351.
- Couchman, H. 1991 ApJ, 368, L23
- Craig, M. 1997 poster presented at "Dynamics and Statistics of Large–Scale Structures in the Universe", University of Kansas.
- Doroshkevich, A.G., Kotok, E., Novikov, I.D., Polyudov, A.N., Shandarin, S.F., & Sigov, Yu.S. 1980 MNRAS 192, 321.
- Efstathiou, G.E., Frenk, C.S., White, S.D.M., & Davis, M. 1988 MNRAS 235, 715.
- Evrard, A.E. & Crone, M.M. 1992 ApJ 394, L1.
- Hockney, R.W. & Eastwood, J.W. 1988 Computer Simulation Using Particles (New York: McGraw-Hall), p. 454
- Kauffmann, G.A.M., and Melott, A.L. 1992 ApJ 393,415.
- Klypin, A.A., Gottlober, S., and Kravtsov, A.V. 1997 astro-ph/9708191
- Kuhlman, B., Melott, A.L., & Shandarin, S.F. 1996, ApJ 470, L41.
- Little, B., Weinberg, D.H., & Park, C.B. 1991 MNRAS, 253, 295.
- Melott, A.L. 1981 Ph.D. Thesis, University of Texas
- Melott, A.L. 1986 Phys Rev Lett, 56, 1992
- Melott, A.L. 1990 Comments Ap. 15, 1
- Melott, A.L., Splinter, R.J., Shandarin, S.F., & Suto, Y. 1997 ApJ, 479, L79
- Moore B., Governato, F., Quinn, T., Stadel, J. and Lake, G. 1997 preprint astro-ph/9709051
- Park, C.B. 1996 B.A.A.S. 189, 122.18.
- Peebles, P.J.E., Melott, A.L., Holmes, M.R., Jiang, L.R., 1989 ApJ, 345, 108

- Ryden, B.S., and Gramann, M. 1991 ApJ 383, L33.
- Splinter, R.J. 1996 MNRAS 281, 281
- Splinter, R.J., Melott, A.L., Shandarin, S.F., and Suto, Y. 1998 ApJ in press astro-ph/9706099
- Suginohara, T., Suto, Y., Bouchet, F.R., & Hernquist, L. 1991, ApJS, 75, 631
- Suisalu, I., & Saar, E. 1995 preprint astro-ph/9511120
- Suto, Y. 1993, Prog. Theor. Phys., 90, 1173
- Yess, C., & Shandarin, S.F. 1996, ApJ, 465, 2
- Zel'dovich, Ya. B. 1970, A&A, 5, 84



Table 1. Model Parameters for the Test Cases

Code		N	$\bar{l}_{sep}$ <sup>a</sup>	$\epsilon_{force}$ <sup>b</sup>
PM	$k_c = 16$	$128^3$	1.0	1.0
	$k_c = 64$	$128^3$	1.0	1.0
P <sup>3</sup> M	$k_c = 16$	$32^3$	4.0	0.25
	$k_c = 16$	$128^3$	1.0	1.0
Tree	$k_c = 16$	$32^3$	4.0	0.25

<sup>a</sup> $\bar{l}_{sep}$  is the mean particle separation in grid cell units.

<sup>b</sup> $\epsilon_{force}$  is in units of the mean particle separation,  $\bar{l}_{sep}$ . Note that for all runs here  $a \equiv \epsilon_{force} \times \bar{l}_{sep} = 1$ .

Table 2. Cross-Correlations at Final Stage

	PM		P <sup>3</sup> M		Tree
	$k_c = 16$	$k_c = 64$	$128^3 \epsilon = 1.0$	$\epsilon = 0.25$	$\epsilon = 0.25$
PM ( $k_c = 16$ )	—	0.65	0.83	0.64	0.52
PM ( $k_c = 64$ )	0.96	—	0.63	0.57	0.47
P <sup>3</sup> M $128^3$ ( $\epsilon = 1.0$ )	0.99	0.95	—	0.66	0.50
P <sup>3</sup> M ( $\epsilon = 0.25$ )	0.96	0.94	0.97	—	0.70
Tree ( $\epsilon = 0.25$ )	0.92	0.90	0.92	0.96	—

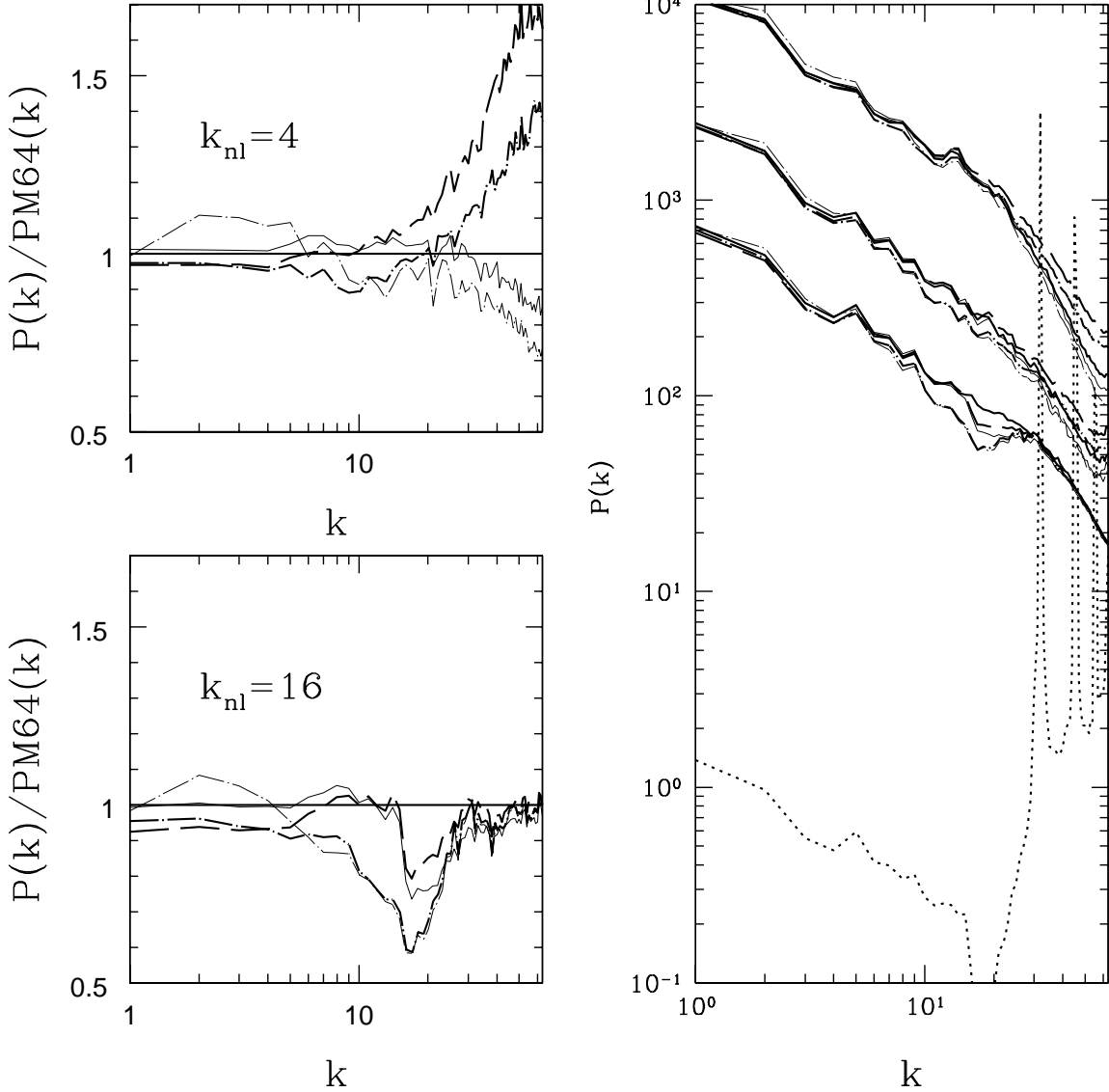


Fig. 1.— Right panel: The power spectrum of our initial conditions and three successive evolved stages for all our simulations, evaluated from  $32^3$  particles on a  $128^3$  mesh (their force resolution). The normalization is such that a Poisson distribution of  $128^3$  particles would converge to  $P = 1$ . The light solid line is the  $k_c = 16k_f$  PM run; the heavy solid line is the  $k_c = 64k_f$  PM run. Other heavy lines are P<sup>3</sup>M runs and light lines are tree code runs. The dotted lines are the initial conditions for the  $32^3$  particle runs; the spikes are discreteness effects due to the finite number of particles. Other lines: Longdash is the P<sup>3</sup>M run with  $128^3$  particles, and the longdash-dot lines are the P<sup>3</sup>M and Tree runs with  $32^3$  particles. Left panel: The ratio of the power in a given model to that in our fiducial  $k_c = 64k_f$  PM run at the first (bottom) and last (top) evolved stage.

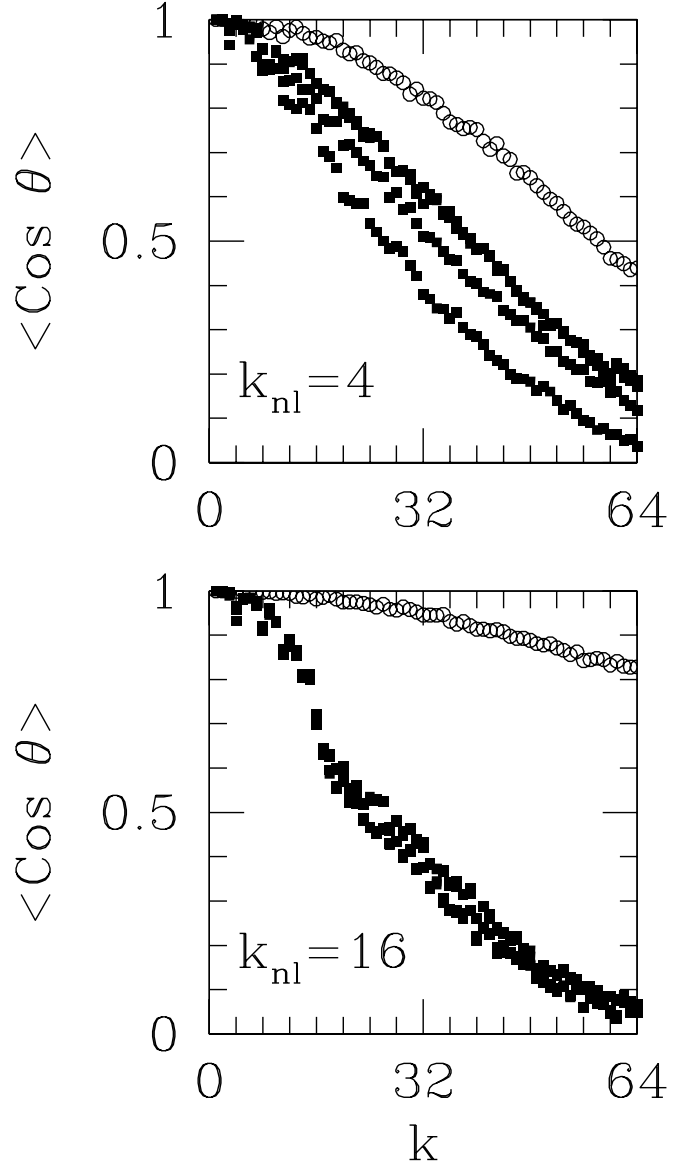


Fig. 2.— The successive plots contain all the data for the averaged phase agreement between *all* of the simulations runs at the same stage;  $\langle \cos \theta \rangle$  is defined in the text and is 1 for agreement and 0 for uncorrelated phases. The filled squares indicate cross-correlation of other runs against the PM run which continued the power-law perturbations to wave-numbers impossible for small numbers of particles ( $k_c = 64k_f$ ). Open circles represent cross-correlation between the  $128^3$  P<sup>3</sup>M run and the PM run with  $k_c = 16k_f$  (also  $128^3$  particles). All other possible cross-correlations here (not shown) lie between these extremes. As before, the top panel is the last evolved stage.

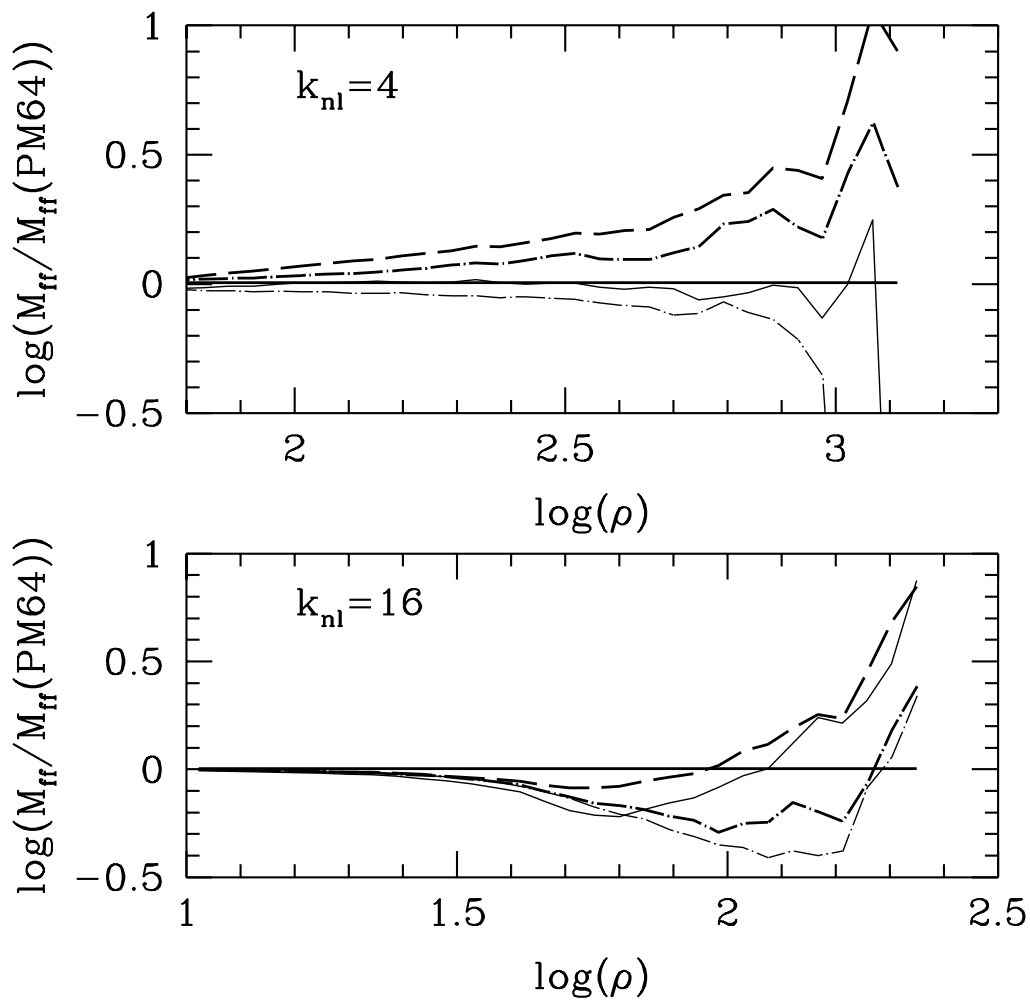


Fig. 3.— The lines (same types as in Figure 1) show the amount of mass in regions of densities greater than the density threshold shown on the horizontal. The densities were calculated on the  $128^3$  mesh. The values are shown as ratios to the fiducial PM model with  $N = 128^3$ , and  $k_c = 64$ , at our earliest evolved stage (bottom) and our latest (top).